HNPS Advances in Nuclear Physics

Vol 9 (1998)

HNPS1998

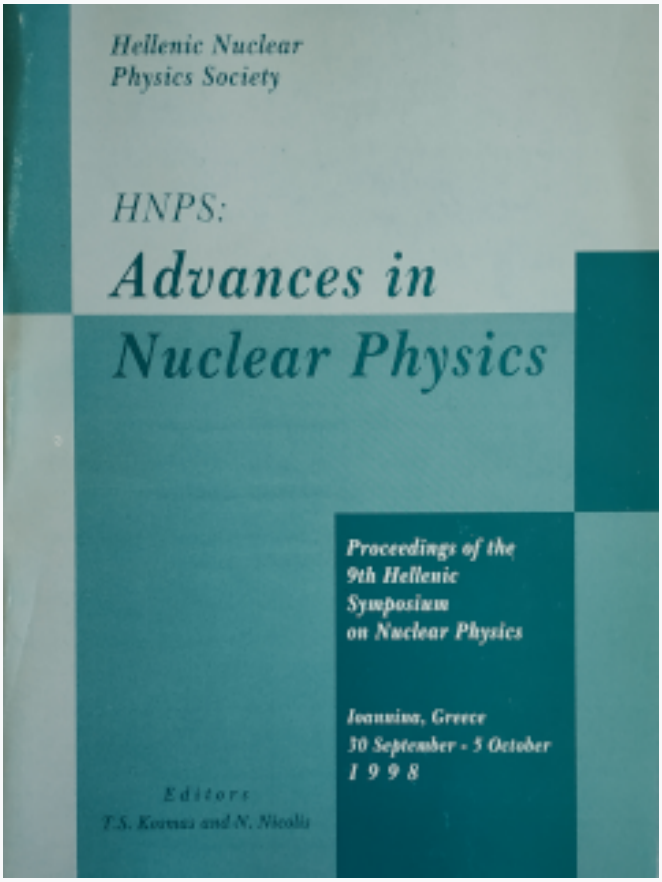

Statistical modeling with neural nets: nuclear masses and halflives

E. Mavrommatis, S. Athanassopoulos, A. Dakos, K. A. Gernoth, J. W. Clark

doi: 10.12681/hnps.2787

Statistical modeling with neural nets: nuclear masses and halflives

E. Mavrommatis [a], S. Athanassopoulos [a], A. Dakos [a], K.A. Gernoth [b], and J.W. Clark [c]

[a] *Physics Department, Division of Nuclear and Particle Physics, University of Athens, GR-15771 Athens, Greece*

[b] *Department of Physics, UMIST, P.O. Box 88, Manchester M60 1QD, United Kingdom*

[c] *McDonnell Center for the Space Sciences and Department of Physics, Washington University, St. Louis, Missouri 63310, USA*

Abstract

Multilayer feedforward neural networks are used to create global models of atomic masses and lifetimes of nuclear states, with the goal of effective prediction of the properties of nuclides outside the region of stability. Innovations in coding and training schemes are used to improve the extrapolation capability of models of the mass table. Studies of nuclear lifetimes have focused on ground states that decay 100% via the β^- mode. Results are described which demonstrate that in predictive acuity, statistical approaches to global modeling based on neural networks are potentially competitive with the best phenomenological models based on the traditional methods of theoretical physics.

1 Introduction

The last decade has seen the development of powerful new methods of statistical analysis, including neural networks adapted to classification and function-approximation tasks [1,2]. In particular, multilayer feedforward neural networks trained on backpropagation and other supervised learning algorithms [3] may be applied to generate a "predictive" statistical model of a given input-output mapping, whether physical or mathematical in character. Information contained in a set of training examples of the input-output association is embedded in the weights of the connections between the layered units. This information may (or may not) be sufficient for the trained network to make reliable predictions for examples outside the training set. Thus, the network

may be taught to generalize, based on what it has learned from the set of examples. In more mundane terms, the model provides a means for interpolation or extrapolation. In scientific or real-world problems, the available data is limited and generally biased, so that success is by no means guaranteed.

Artificial neural networks have been employed to construct predictive statistical models in a variety of scientific settings from astronomy to experimental high- energy physics to protein structure [2]. Nuclear physics offers especially rich territory for "data mining" with neural nets. For one thing, there is available a huge collection of high-quality experimental data on diverse properties of more than 2000 nuclides. For another, quantitative calculation of some properties of some classes of nuclei presents difficult challenges even for the best *ab initio* quantum-mechanical theories and microscopic phenomenological models. To date, global neural-network models have been successfully developed for the stability/instability dichotomy, for the atomic-mass table, for neutron separation energies, for spins and parities, and for decay branching probabilities of nuclear ground states [6-9,4,5]. In the present work, we report new results from exercises in neural-network modeling of atomic masses and the halflives of unstable nuclear ground states that decay 100% via the β^- mode.

The problem of devising global models of nuclidic (atomic) masses has a long history, going back to the early work of Bohr, von Weizsäker, and Bethe based on the liquid drop model. (For recent reviews, see refs. [10,11].) The primary aims are (i) a fundamental understanding of the physics of the mass surface and (ii) the prediction of the masses of "new" nuclides far from stability – both in the superheavy region and in the regions approaching the proton and neutron drip lines. Neural networks can contribute to the realization of the second aim if not the first. The predicted masses are of great current interest in connection with present and future experimental studies of nuclei far from stability, conducted at heavy-ion and radioactive ion-beam facilities [12]. The results are also useful in such astrophysical problems as nucleosynthesis and supernova models. The existing global models of the mass table lie on a spectrum extending from low to high theoretical input (and correspondingly, high to low numbers of fitting parameters). Extrapability of such models is measured by the accuracy of mass prediction for new nuclides not involved in the fitting process, relative to the accuracy of the model for the fitted nuclei (or nuclei belonging to the training set). Neural network mass models, as currently developed, rely on minimal theoretical input. The current work is a continuation of the program established in refs. [6,7,9], with improvement of certain aspects of coding and training.

Regardless of the methods employed, prediction of the β-decay lifetimes of neutron-rich nuclei (or "new" nuclei generally) is of great current interest from several perspectives, including main-stream nuclear physics, nuclear astrophysics, and nuclear technology [13]. Models rooted in quantum theory and

involving large-scale computations have been developed and tested in refs. [14–17]. These models necessarily entail simplifications and approximations, with the consequence that the results for β^- halflives sometimes deviate from experiment by more than a factor 10. The neural-network statistical approach offers a promising alternative to this more traditional treatment. Successful multilayer neural network models of β-decay systematics have already been described in ref. [19]. Here we expand upon that work, presenting models trained with additional experimental input, notably the Q-value of the decay process.

2 Masses

With regard to global modeling of the atomic-mass surface, our primary concern has been the training of neural nets to predict the mass excess ΔM. In constructing some of the models, we have taken account of the experimental errors associated with the mass values used for the training set, applying the "cleanprop" algorithm developed in ref. [9]. Additionally, we have made attempts to create an informative statistical model of the *differences* between the experimental mass excess values ΔM^{exp} and the theoretical values ΔM^{th} generated by the macroscopic-microscopic model of Möller et al. [20]. The latter study is being carried out with the hope of revealing subtle regularities of nuclear structure not yet embodied in the best microscopic/phenomenological models of atomic-mass systematics. Any significant findings of this study will be reported elsewhere; here we focus on new results from direct neural-network modeling of ΔM.

2.1 Design and training of neural-network mass models

We employ multilayer feedforward networks of various architectures. The (gross) architecture of a given net is summarized in the notation $(I\text{–}H_1\text{–}H_2\text{–}...\text{–}H_L\text{–}O)[P]$, where P is the total number of weight/bias parameters and I, H_i, and O are integers that indicate, respectively, the numbers of neuron-like units in the input layer, ith intermediate (or "hidden") layer, and the output layer. Except when pruning is implemented to eliminate unimportant weights (see below), all forward connections from each layer to the next are present. The activation function of the neuronal units is taken to be the logistic function. The model networks are trained with a *modified* version of the familiar back-propagation algorithm [3] that proves in most cases to be more efficient in avoiding local minima of the cost function or objective function that the learning algorithm is nominally intended to minimize. As in standard (or "vanilla") back-propagation, the weight-update rule contains a momentum term that has

an inertial effect on the search path, damping out wild oscillations when deep, narrow troughs of the cost surface are encountered [18]. However, the momentum term is modified to introduce a recursive process such that weight changes extending far back in time – not just the most recent change – are allowed to influence the current update. On-line rather than batch updating is implemented. Thus, weights are updated after presentation of each example rather than after completion of each epoch, i.e., after each pass through the randomly-sequenced training corpus. To improve the quality of the trained model, strategic changes of both the learning rate and momentum parameter are made during the training process. The training stops when the lowest value of the cost function has been achieved in the validation set. In some cases, pruning of weights of lesser importance is carried out, followed by retraining (cf. ref. [7]); this generally results in better predictive accuracy without serious sacrifice of performance on the training set.

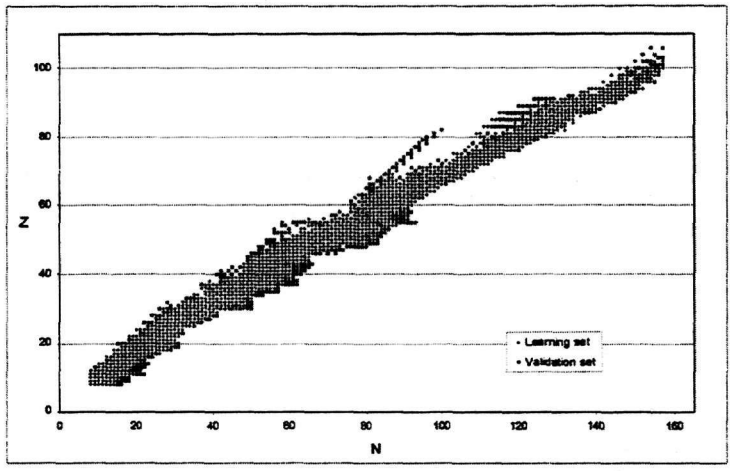

Fig. 1. Locations in the $N - Z$ plane are shown for the 1323 ("old") nuclei of the training set and the 351 ("new") nuclei of the validation set used in neural-network modeling of the special Möller-Nix (MN) mass-excess database.

We report results obtained using a special database consisting of 1323 "old" (O) experimental masses that the 1981 Möller-Nix model [21] was designed to reproduce, together with 351 "new" (N) mass data that lie mostly beyond the edges of the 1981 data set as viewed in the $N - Z$ plane. The locations of old and new nuclei are shown in Fig. 1. This database (designated MN for short) was formed by Möller and Nix [10] to assess the extrapolation capability ("extrapability") of different global models of atomic masses. In creating neural-network models, the old masses are used as the training set and the new masses provide a validation or prediction set.

Three different input coding schemes have been studied. In the first [6,7], the input layer consists of sixteen on-off units (eight for Z, eight for N) that serve to encode the proton and neutron numbers in *binary*. This scheme facilitates learning of quantal properties (pairing, shell structure) that depend on the integral nature of Z and N. The second scheme implements *analog* coding of Z, N in terms of the activities of only two analog input neurons, which, however, are aided by two further on-off input units that code for the parity (even or odd) of Z and N. (Thus the network is again given information about the integral character of Z and N.) In the third scheme, the 16-unit binary-coding input array of the first design is supplemented by two additional units encoding Z and N in analog. In any of these cases, the mass excess computed by the network is represented by the activity of a single analog output unit. As performance measures in learning, validation and prediction sets we use the root-mean-square (rms) deviation from experiment, denoted σ_{rms}, as well as the number of patterns (examples) for which the value got in the output deviates from experiment by less or equal than 5%. The rms error is widely adopted as the figure of merit in global modeling of the mass table.

Table 1

Comparison of neural network models of mass-excess data with other models based on nuclear theory
Use is made of data basis MN [1323(O) - 351(N)]

Net type of model (I-H_1-...-H_2-O) [P]	Learning mode $\sigma^{[e]}=\sigma_{RMS}$	Recalled Patterns	Validation (v) & Prediction (p) mode $\sigma^{[e]}=\sigma_{RMS}$	Recalled Patterns
(16-10-10-10-1) [401] Z & N in binary	0.393	1172/1323	3.575 (v)	246/351
(18-10-10-10-1) [421] Z &N in binary and decimal	0.331	1187	2.199 (v)	272
(4-10-10-10-1)* [281] Z & N in decimal and parity	0.491	1141	1.416 (v)	280
(4-10-10-10-1)** [273] Z & N in decimal and parity	0.617	1095	1.209 (v)	284
(4-40-1) [245] [a]	1.068	-	3.036 (p)	-
Möller et al. [b]	0.673	-	0.735 (p)	-

a) **B. L. Kalman**, see ref.[22]

b) **P. Möller, J. R. Nix**, see ref.[10]

2.2 Results

Some results from our computer explorations are reported below in Tables 1 and 2 and Fig. 2. As shown in Table 1, the best model for the MN mass-excess database, marked with two asterisks, has gross architecture (4–10–10–10–1). This net is a descendent, via the pruning procedure, of the network of the same gross architecture marked with one asterisk. Performance of these networks is compared with that of two others employing binary encoding at the input and with that of a three-layer net constructed by Kalman [9,22]. Most interesting is

the comparison with the rms error measures obtained in state-of-the-art treatments based on the macroscopic-microscopic model of Möller et al. [10,20]. A strong test is provided by 10 rare-earth nuclides situated beyond the edges of the two subsets (O) and (N) of the MN database. (The mass defects of these nuclides have recently been measured with the ISOLTRAP mass spectrometer [23].) As explained above, performance on the data subset (N) was used to determine the stopping point for training. Accordingly, this set has a nontrivial effect on the construction of the network model and does not qualify as a pristine prediction set in the usual sense. However, the 10 "newer" nuclides do so qualify. Table 2 presents results obtained for these nuclides using the network (4–10–10–10–1)**. The corresponding value of $\sigma_{\rm rms}$ is $0.820 MeV$, which compares quite favorably with the value $0.500 MeV$ quoted in ref. [20] for the FRDM macroscopic/microscopic model. Relative to neural-network modeling results reported earlier [7], the best of the current models represent a dramatic step toward extrapability levels competitive with those reached by the best traditional global models rooted in quantum theory. With further improve-

Table 2

Illustration of the power of the neural network model (4-10-10-10-1) to predict the values of the mass excess ΔM of 10 rare earth nuclides beyond the edges of the MN database. Comparison is been made with the experimental values (measured with ISOLTRAP [21]) as well as with the results of the FRDM model of Moller et al. [20]. The root mean square deviation σ_{RMS} is found equal to *0.820* and to *0.500 MeV* for the neural network and the FRDM model respectively.**

Nuclide	Z	A	Experimental values (MeV)	Predicted values (MeV)	FRDM values (MeV)
Ba	56	123	-75.66	-73.89	-75.60
Pr	59	133	-77.94	-77.46	-77.64
Pr	59	134	-78.51	-78.56	-78.10
Nd	60	132	-71.40	-70.00	-71.49
Nd	60	134	-75.65	-75.01	-75.13
Nd	60	138	-82.02	-82.60	-81.01
Pm	61	138	-74.92	-75.50	-74.29
Sm	62	136	-66.81	-66.43	-66.52
Sm	62	138	-71.50	-71.50	-70.83
Eu	63	139	-65.40	-65.82	-65.27

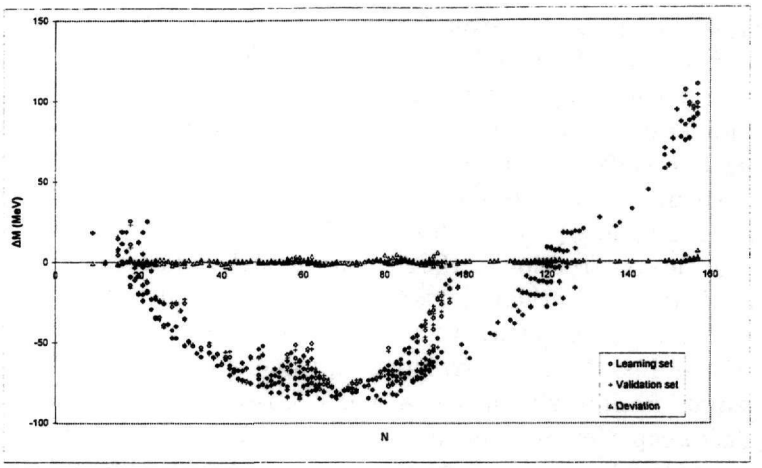

Fig. 2. Values of the mass excesses (in Mev) predicted by the neural-network model (4–10–10–10–1)** for the validation set corresponding to Fig. 1 are compared with experiment. The plot represents a projection of the mass surface onto a plane of constant Z and thus displays dependences on the neutron number N.

ments (see for ex. ref. [18]) that appear to be feasible, it may be expected that statistical modeling will provide a valuable tool for predicting atomic masses far from stability.

3 Halflives

We now turn to the application of neural-network statistical methodology to the systematics of nuclear decay. Attention is restricted to the important problem of predicting the halflives $T_{\frac{1}{2}}$ of nuclear ground states that decay 100% by the β^- mode.

3.1 Design and training of neural-network half-lives models

Since the relevant experimental halflives vary over 26 orders of magnitude, the target variable for prediction is taken to be $\ln T_{\frac{1}{2}}$. Vanilla backpropagation, involving a mean-square cost function, logistic activation functions, and a momentum term in the update rule is employed for on-line training of multilayer feedforward models. Each training run involves a pre-set number of epochs, and the weights that are kept after each run are taken as those yielding the best value of the performance measure $< x >_K$ achieved during the run. (This performance measure is identified below.)

Three different databases were used in our computational study:

(i) Database A, formed from all data available in early 1995 from the Brookhaven National Nuclear Data Center, encompassing a total of 766 nuclides with β^- half-lives ranging from 0.15×10^{-2} sec for $^{35}_{11}$Na to 0.2932×10^{24} sec for $^{143}_{48}$Cd. Of the 766 examples, 575 are selected (at random) for the training set, with the remaining 191 used as a test set.

(ii) Database A–10^6, formed from basis A by removing nuclides with $T_{\frac{1}{2}}$ values greater than 10^6 sec. This set contains 697 nuclides, a randomly chosen set of 523 being employed for learning and the remaining 174 for prediction.

(iii) Database B, obtained from Database A-10^6 by omitting a few isomeric decays, leaving 692 nuclides of which 518 are reserved for learning and 174 for prediction (see Fig. 3).

These databases are chosen to allow reasonable comparisons to be made with the results from traditional global models of β^- halflives [15–17].

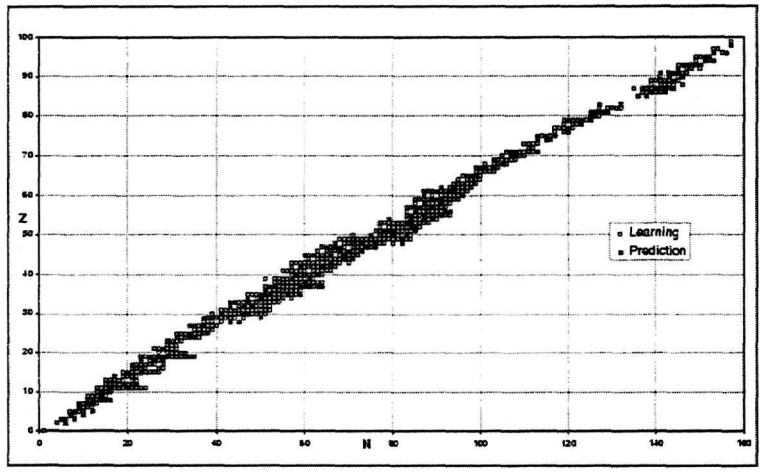

Fig. 1. Location, in the $N - Z$ plane, of the nuclides of database B. The distinction between nuclides belonging to training and prediction sets used for neural-network modeling are indicated.

In most cases, we utilize binary coding of Z and N at the input layer, in the same arrangement as employed in some of the mass models. In several cases, we append an additional input unit that encodes, in analog, the Q value of the decay. A single analog output unit generates the coded value of $\ln T_{\frac{1}{2}}$ that the network associates with the input nuclide.

Network performance in learning and prediction is measured in terms of (i) the root-mean-square deviation $\sigma_{\rm rms}$ of the calculated value of $\ln T_{\frac{1}{2}}$ from its experimental value; (ii) the deviation $< x >_K$ and associated standard deviation σ_K introduced by Klapdor-Kleingrothaus and adopted in refs. [14–16]; and the deviation $< x >_M$ and associated standard deviation σ_M used by Möller et al. [17]. As a further performance measure, we have examined the percentage m of those nuclides whose ground-state β^- halflives $T_{\frac{1}{2}}^{\rm exp}$ lie within a prescribed range (e.g. not greater than 10^6s, 60s, and 1s), for which the half-life generated by the network is within a prescribed tolerance factor (2 or 10) of the experimental value.

Table 3

Quality measures in learning and prediction of half-lives of β^-decaying nuclides by feedforward neural networks of various types trained with back-propagation algorithm for 20000 epochs.

Net type	Data	Learning Mode		Prediction Mode	
(I-H_1-...-H_L-O) [P]		Nuclides	σ_{RMS}	Nuclides	σ_{RMS}
(16-10-1) [181]	A - all	575	3.792	191	4.969
	A - 10^6 sec	523	1.079	174	1.819
(16-10-10-1) [291]	A - all	575	0.974	191	5.864
	A - 10^6 sec	523	0.646	174	2.264
(16-10-1) [181]	B - 10^6 sec	518	1.099	174	2.072
(17-10-1) [191] Q values	B - 10^6 sec	518	0.772	174	1.882
(16-10-10-1) [291]	B - 10^6 sec	518	0.528	174	3.020
(17-10-10-1) [301] Q values	B - 10^6 sec	518	0.455	174	2.894

Results with Database A are reported in ref. [19]

Table 4

Illustration of the power of the neural network model [17-10-1] in the learning mode to yield the values of β^- decay half-lives and comparison with the results of Staudt et al. [15] and Homma et al. [16]

		Learning			Staudt et al. [15]			Homma et al. [16]	
factor	$T_{\frac{1}{2}}^{\rm exp}$(sec)	m (%)	$<x>_K$	σ_K	m (%)	$<x>_K$	σ_K	m (%)	$<x>_K$
≤10	$<10^6$	99.4	2.03	1.16	72.2	1.85	1.21	76.7	3.00
	<60	100	1.98	1.09	96.3	1.67	1.02	87.2	2.81
	<1	100	2.04	1.10	99.1	1.44	0.40	95.7	2.64
≤2	$<10^6$	65.8	1.40	2.67	56.4	1.37	0.29	33.8	1.43
	<60	64.8	1.40	2.59	82.2	1.36	0.29	42.0	1.41
	<1	59.2	1.37	2.72	90.0	1.35	0.27	50.7	1.43

Table 5

Illustration of the power of the neural network model [17-10-1] in the learning and prediction mode to yield the values of β^- decay half-lives and comparison with the results of Moller et al. [17] and Homma et al. [16]

		Learning			Prediction			Moller et al. [17]			Homma et al. [16]		
$T_{1/2}^{exp}$ (sec)		n	M^{16}	σ^{16}	n	M^{16}	σ^{16}	n	M^{16}	σ^{16}	n	M^{16}	σ^{16}
<1	o-o	32	1.15	2.27	10	2.05	2.31	29	0.59	2.91	28	1.75	4.96
	o-e	52	1.07	2.03	20	1.08	2.38	35	0.59	2.64	31	0.60	2.24
	e-e	19	1.61	1.71	5	1.79	2.71	10	3.84	3.08	10	1.15	2.36
<10	o-o	67	1.17	2.25	18	2.26	5.42	59	0.76	8.83	66	1.89	4.60
	o-e	101	1.04	1.91	30	1.19	2.44	85	0.78	4.81	81	0.92	3.84
	e-e	43	1.19	2.09	12	1.31	2.30	34	2.50	4.13	34	1.01	2.93
<100	o-o	92	1.18	2.18	39	1.76	5.19	88	2.33	49.19	85	3.15	10.51
	o-e	156	1.05	1.93	58	1.12	3.15	133	1.11	9.45	127	1.07	4.29
	e-e	59	1.19	1.97	25	0.98	2.67	54	2.61	4.75	52	1.13	3.58
<1000	o-o	110	1.19	2.13	52	2.22	6.25	115	3.50	72.02	93	3.02	10.25
	o-e	204	0.98	1.99	91	1.22	5.50	194	2.77	71.50	157	1.10	5.55
	e-e	73	1.14	1.95	31	0.93	4.78	71	6.86	58.48	63	1.39	6.10

3.2 Results

Selected results of our simulations are collected in Table 3. The results for Database A basis have already been reported in ref. [19]. Among nets trained on Database B, the best in predictive performance is that with architecture (17–10–1)[191] having binary (Z,N) and analog Q inputs. In Tables 4 and 5, we compare the performance measures for this particular network with those of the conventional global models of Staudt et al. [15], Homma et al. [16], and Möller et al. [17]. The level of performance displayed by the network model is similar to (and in some cases better than) that of the latter models. Two qualifications should accompany any assessment of the relative merits of neural-network and traditional approaches. On the one hand, comparison is hindered by the absence of a clear distinction between the aspects of fitting and prediction in the conventional treatments; and on the other, the neural-network model has many more adjustable parameters than the traditional models. At any rate, the good performance of the (17–10–1) network model is clearly demonstrated in Fig. 4, where the experimental halflives of isotopes of Cu are plotted against neutron number N, along with halflives generated by the net. In Fig. 5, the results given by this network for nuclides on or near the r-process path are compared with experiment. The encouraging results of these and other computer studies provide a strong incentive for seeking further improvements of network performance and extending the approach to other decay modes, notably β^+ decay.

Acknowledgements

This research was supported in part by the US National Science Foundation under Grant No. PHY-9900713 and the University of Athens under Grant No. 70/4/3309.

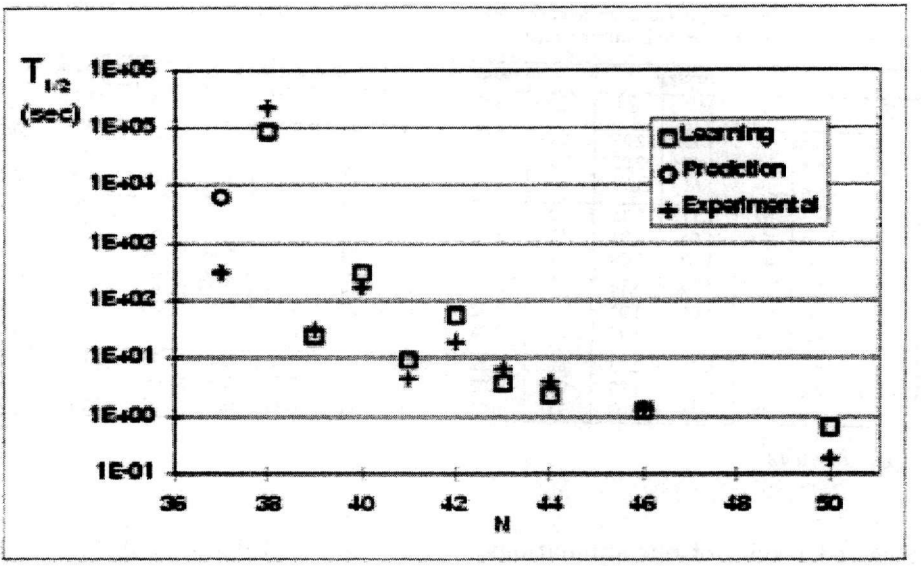

Fig. 2. Experimental and calculated β^- halflives of Cu isotopes, plotted versus neutron number N. The calculated results are generated by the network model (17–10–1) and represent fits or predictions, depending, respectively, on whether a given isotope belongs to the training or prediction set.

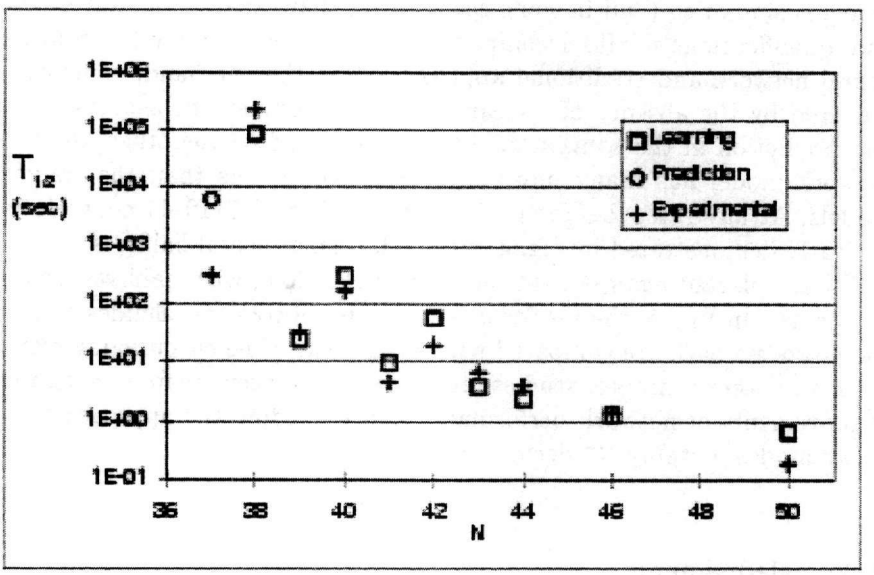

Fig. 3. Experimental and calculated β^- halflives of nuclides that lie on or near the r-process path. The calculated results are generated by the network model (17–10–1) and represent predictions for ^{130}Cd and ^{131}In and fits for the other examples.

References

[1] V. Cherkassky, J. H. Friedman, and W. Wechsler, eds., *From Statistics to Neural Networks. Theory and Pattern Recognition Applications* (Springer-Verlag, Berlin, 1994)

[2] J. W. Clark, T. Lindenau, and M. L. Ristig, eds., *Scientific Applications of Neural Nets* (Springer-Verlag, Berlin, 1999)

[3] J. Hertz, A. Krogh and R. G. Palmer, *Introduction to the Theory of Neural Computation* (Addison-Wesley, Redwood City, CA, 1991); J. W. Clark, Phys. Med. Biol. **36** (1992) 1259; S. Haykin, *Neural Networks: A Comprehensive Foundation* (McMillan, New York, 1993); C. Bishop, *Neural Networks for Pattern Recognition* (Clarendon, Oxford, 1995)

[4] J. W. Clark, in *Scientific Applications of Neural Nets*, J. W. Clark, T. Lindenau, and M. L. Ristig, eds. (Springer-Verlag, Berlin, 1999), p. 1

[5] K. A. Gernoth, in *Scientific Applications of Neural Nets*, J. W. Clark, T. Lindenau, and M. L. Ristig, eds. (Springer-Verlag, Berlin, 1999), p. 139

[6] S. Gazula, J. W. Clark and H. Bohr, Nucl. Phys. **A540** (1992) 1

[7] K. A. Gernoth, J. W. Clark, J. S. Prater and H. Bohr, Phys. Lett. **B300** (1993) 1

[8] K. A. Gernoth and J. W. Clark, Neural Networks **8** (1995) 291

[9] K. A. Gernoth and J. W. Clark, Comp. Phys. Commun. **88** (1995) 1

[10] P. Möller and J. R. Nix, J. Phys. G **20** (1994) 1681

[11] **a)** C. Borcea and G. Audi, Rom. J. Phys **38** (1993) 455; **b)** G. Audi, O. Bersillon, J. Blachot and A. H. Wapstra, Nucl. Phys. **A624** (1997) 1

[12] *Nuclear Science: A Long Range Plan* DOE/NSF (1996); *Nuclear Physics in Europe: Highlights and Opportunities* NUPECC (1997)

[13] H. V. Klapdor, Prog. Part. Nucl. Phys. **10** (1983) 131

[14] H. V. Klapdor, J. Metzinger and T. Oda, At. Data Nucl. Data Tables **31** (1984) 81

[15] A. Staudt, E. Bender, K. Muto, H. V. Klapdor - Kleingrothaus, At. Data Nucl. Data Tables **44** (1990) 79

[16] H. Homma, E.Bender, M. Hirsch, K. Muto, H. V. Klapdor-Kleingrothaus and T. Oda, Phys. Rev. **C54** (1996) 2972

[17] P. Möller, J. R. Nix and K. L. Kratz, At. Data Nucl. Data Tables **66** (1997) 131

[18] S. Athanassopoulos, E. Mavrommatis, K. A. Gernoth, and J. W. Clark, to be submitted for publication.

[19] E. Mavrommatis, A. Dakos, K. A. Gernoth and J. W. Clark, in *Condensed Matter Theories*, Vol. 13, ed. by J. da Providência and F. B. Malik (Nova Science Publishers, Commack, NY 1998) 423

[20] P. Möller, J. R. Nix, W.D. Myers and W. J. Swiatecki, Nucl. Phys. **A536** (1992) 61; P. Möller, J. R. Nix, W. D. Myers, and W. J. Swiatecki, At. Data Nucl. Data Tables **59** (1995) 185

[21] P. Möller and J. R. Nix, At. Data Nucl. Data Tables **26** (1981) 165

[22] B. L. Kalman, private communication.

[23] D. Beck et al., Nucl. Phys. **A626** (1997) 343c